Computer Methods and Programs in Biomedicine 224 (2022) 107022

Contents lists available at ScienceDirect

Computer Methods and Programs in Biomedicine

journal homepage: www.elsevier.com/locate/cmpb

A novel online BCI system using speech imagery and ear-EEG for home appliances control

Netiwit Kaongoen[1], Jaehoon Choi[1], Sungho Jo*

School of Computing, Korea Advanced Institute of Science and Technology, Daejeon, South Korea

ARTICLE INFO

Article history:
Received 25 March 2022
Revised 30 June 2022
Accepted 11 July 2022

Keywords:
Brain-computer interface
Speech-imagery
Ear-EEG

ABSTRACT

Background and Objective: This paper investigates a novel way to interact with home appliances via a brain-computer interface (BCI), using electroencephalograph (EEG) signals acquired from around the user's ears with a custom-made wearable BCI headphone.
Methods: The users engage in speech imagery (SI), a type of mental task where they imagine speaking out a specific word without producing any sound, to control an interactive simulated home appliance. In this work, multiple models are employed to improve the performance of the system. Temporally-stacked multi-band covariance matrix (TSMBC) method is used to represent the neural activities during SI tasks with spatial, temporal, and spectral information included. To further increase the usability of our proposed system in daily life, a calibration session, where the pre-trained models are fine-tuned, is added to maintain performance over time with minimal training. Eleven participants were recruited to evaluate our method over three different sessions: a training session, a calibration session, and an online session where users were given the freedom to achieve a given goal on their own.
Results: In the offline experiment, all participants were able to achieve a classification accuracy significantly higher than the chance level. In the online experiments, a few participants were able to use the proposed system to freely control the home appliance with high accuracy and relatively fast command delivery speed. The best participant achieved an average true positive rate and command delivery time of 0.85 and 3.79 s/command, respectively.
Conclusion: Based on the positive experimental results and user surveys, the novel ear-EEG-SI-based BCI paradigm is a promising approach for the wearable BCI system for daily life.

1. Introduction

A brain-computer interface (BCI) records and translates brain activity into digital commands. It works as a gateway between the human brain and external devices, enabling users to communicate or control environments solely with thoughts, which greatly benefits physically challenged individuals such as those who suffer from amyotrophic lateral sclerosis (ALS) [1]. Most BCIs rely on brain activities acquired from users while performing a specific mental task. For example, P300-based BCIs detect an event-related potential (ERP) from simultaneously monitored electroencephalogram (EEG) to identify the target that a user is mentally concentrating at [2,3]. Motor-imagery (MI) is one of the most popular types of mental tasks employed in BCI systems. During a MI task, a user actively imagines a body movement without actually moving, which causes changes in brain activity in the specific parts of the motor cortex that can be detected by BCI systems [4,5].

Speech-imagery (SI) is a relatively new paradigm in BCI research. Similar to MI, SI tasks involve imagining speaking some specific words without actually producing any sound [6]. Unlike other mental tasks that are commonly used in BCIs, SI tasks are more intuitive to most people which makes SI-based BCIs easier to use with less practice time. It can also be more straightforward; the speech commands can be selected to match their semantic meaning with the actual output commands. For instance, users can imagine the word "Power" to turn on a television. There are two brain regions located in the left cerebral hemisphere that are commonly associated with different language processing functions: Broca's and Wernicke's areas, where the former is involved in language production and the latter in language comprehension [7,8]. Analysis of brain activities in previous works has indicated

* Corresponding author.
E-mail address: shjo@kaist.ac.kr (S. Jo).
[1] Both authors equally contributed to this work.

https://doi.org/10.1016/j.cmpb.2022.107022
0169-2607/

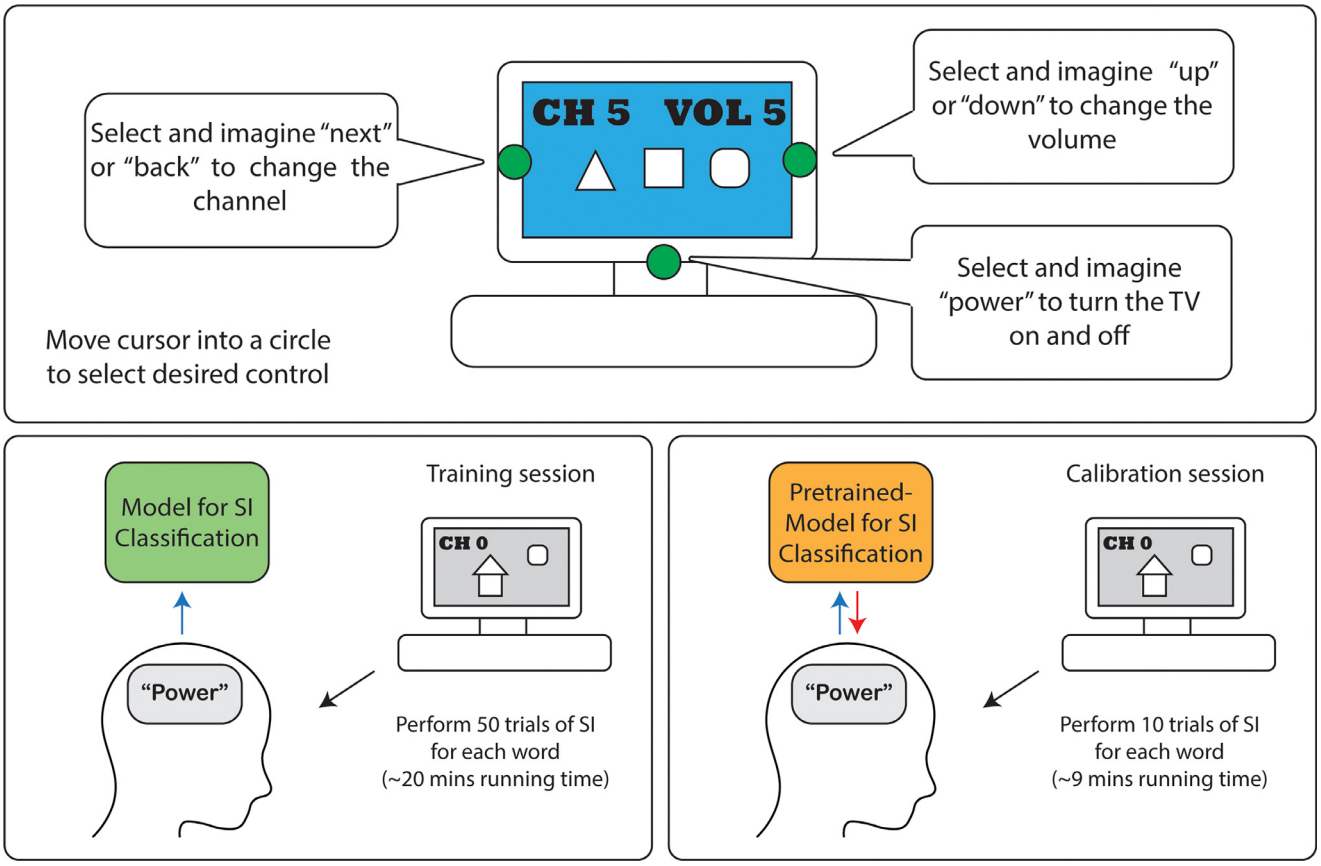

Fig. 1. Overview of the proposed ear-EEG SI-based BCI system for home appliances control. Users initially perform a training session to train the classification models. Subsequently, users can carry out a shorter calibration session to fine-tune the trained models.

an increment in the brain activities in these areas during SI tasks [9,10], suggesting that both phonetic and semantic components of the imagined word influence brain patterns during SI tasks. Various researches have been carried out in an offline setting to show the effectiveness of SI as a potential paradigm for BCI systems, using different types of speech. Some studies focused on using a single phoneme with no semantic meaning [11–13], while others analyzed the classification performance for words with the same or different number of phonemes [10,14–16]. These previous researches demonstrated the potential of SI to be used as a paradigm in BCI systems.

Among brain monitoring techniques, EEG is most commonly employed in non-invasive BCIs due to its temporal resolution, versatility, and cost-efficiency. EEG is conventionally acquired using wet electrodes, with electrolyte gel applied to decrease impedance between the scalp and the electrodes. However, such methods are unsuitable for daily life due to several reasons including their time-consuming preparation process and unpleasant user experience [17]. To solve this issue, there are various ways to adjust EEG acquisition techniques to make BCI wearable. First, wet electrodes that are sticky to the user's hair and skin can be replaced by dry electrodes. AgCl spike-shape dry electrodes are commonly used to ensure contact with the user's scalp even in the presence of hair. Second, the equipment can be made wireless and portable, which is preferable for daily life where users normally have to move around. Third, instead of using an EEG cap, the equipment can be aesthetically redesigned to be worn easily and less socially awkward. Examples of companies that offer commercial-grade wearable EEG headsets include NeuroSky (MindWave headset), Emotiv (offer various types of EEG headset), and InteraXon (Muse headband).

In addition to the above techniques, ear-EEG has been gaining more attention in the wearable BCI research field over the recent years. Ear-EEG is an EEG acquisition technique that monitors EEG from around [18] or inside the user's ears [19]. It is more discreet than the conventional scalp-EEG methods. Moreover, the skins around (and inside) the user's ears are not covered with hair; thus, it is easier to ensure the contact between electrodes and the user's skin for both dry and wet electrodes. Previous studies have proven that ear-EEG is a reliable EEG acquisition method for many types of BCI systems including P300 [18,20], SSVEP [20,21], auditory-steady-state response (ASSR) [20], sleep staging [18], and emotion recognition [22].

Considering the merits of both the SI mental tasks and ear-EEG acquisition method, we propose a novel BCI system that combines SI mental tasks and wearable ear-EEG equipment to further develop BCI for daily life. In our previous work [23], multi-class SI experiments were conducted while recording both conventional scalp-EEG (32 channels) and ear-EEG (6 channels) simultaneously. The results of the offline experiments indicated no significant difference between the performance of the scalp-EEG and ear-EEG in most of the participants, showing that ear-EEG can be used as an alternative EEG acquisition method in SI-based BCIs. This current work builds on the previous work to develop a SI-based BCI system with wearable ear-EEG equipment that can be used for control. The system is evaluated with experiments in both offline and online manner. Ear-EEG is monitored in eight channels positioned around the user's ears using a fully-wearable device shaped similarly to a headphone. The system extracts features from the ear-EEG by applying common spatial pattern (CSP) filters and Riemannian tangent space projections to the covariance matrices calculated from ear-EEG. A multilayer extreme learning machine (MLELM) is then

used to translate the data into corresponding output commands. The proposed system and the experimental protocols are described in detail in the following section.

2. Method and experiment

2.1. System overview

In this work, we propose a novel wearable ear-EEG SI-based BCI for controlling home appliances. Interactive simulated television is made and used as the target home appliance for the experiments. The user is provided with three different ways to control the television, which can be selected by moving the mouse cursor into the respective circle. The user can change the channel (left circle, by performing SIs of words "next" and "back"), change the volume (right circle, by performing SIs of words "up" and "down") and turn the TV on and off (bottom circle, by performing SI of word "power"). Three different classification models are used for each control task. Initially, the user has to perform a training session to train these models, which takes approximately 20 min to complete. For subsequent use, the user can carry out an additional calibration session instead, which takes around 9 min. Fig. 1 depicts the system overall.

The process of our ear-EEG SI-based BCI system begins with acquisitions of ear-EEG data using a custom-made wearable ear-EEG headphone. The ear-EEG data are then preprocessed and bandpass filtered into multiple frequency bands after which the CSP algorithm is applied to spatially filter the data from each frequency band independently. Subsequently, covariance matrices are calculated from the resulting EEG data and projected into the corresponding tangent space according to their Riemannian geometry. Finally, a feature vector is constructed from the transformed covariance matrices and classified using a MLELM model to give an output command that controls the target. Fig. 2 summarizes the whole process of our system in a schematic diagram.

2.2. Participants

Eleven individuals (Nine males and two females) of age ranging from 20 to 30 years old were recruited to participate in this study. All participants were healthy and did not have any neurological, visual, or auditory disorders. Nine participants have prior experiences using BCI systems and six of them have previously participated in a SI-based BCI experiment. All participants gave written consent and the institutional review board (IRB) has approved the study.

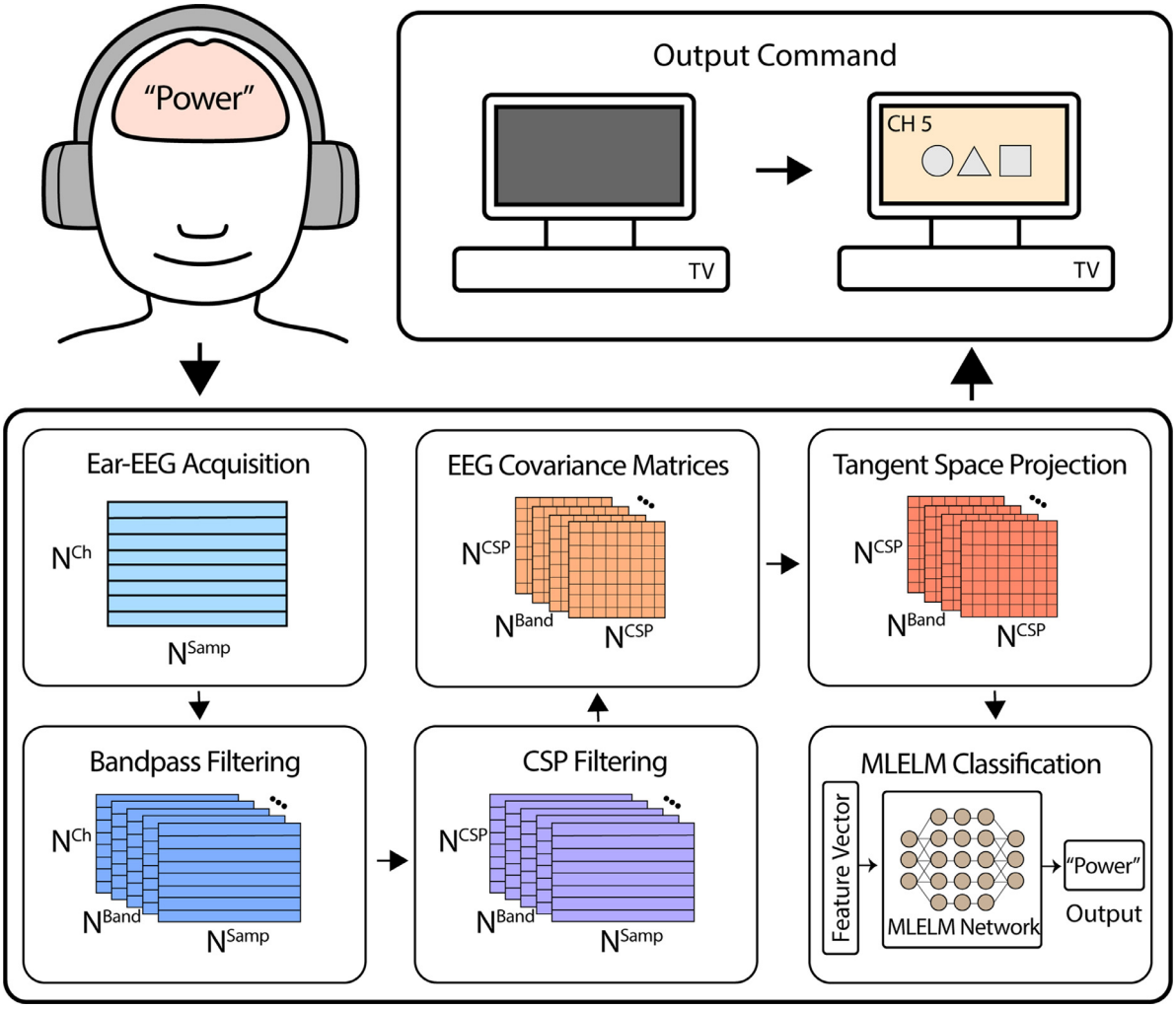

Fig. 2. The schematic diagram of our ear-EEG SI-based BCI system. Ear-EEG data is acquired using a custom-made ear-EEG headphone. The data are processed using mutiple bandpass and CSP filters. The feature extraction is based on Riemannian tangent space projection of the EEG covariance matrix. MLELM is used as the classifier that outputs a command that controls the state of the target.

(a) (b)

Fig. 3. The front-view (a) and side-view (b) of the custom-made wearable ear-EEG headphone.

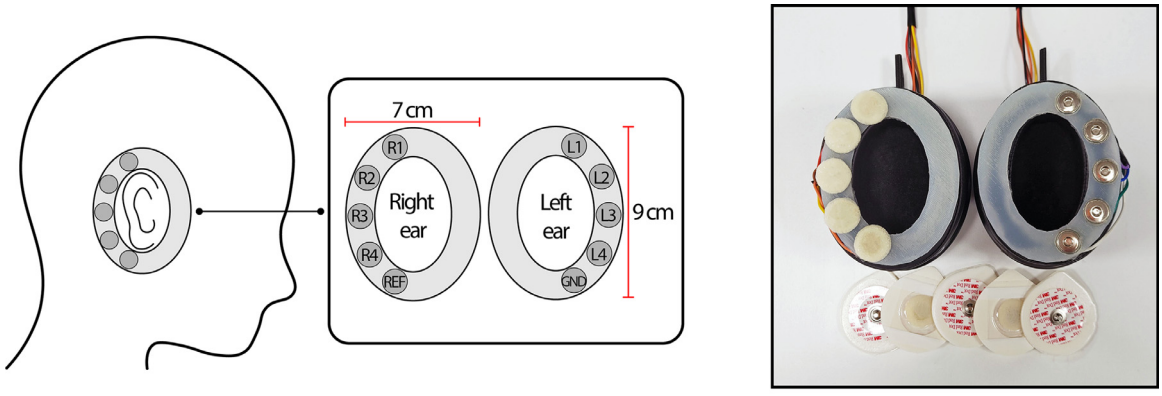

(a) (b)

Fig. 4. The positions of the ear-EEG electrodes at both ears (a) and the actual photo of the headphone cups with electrodes attached to the left cup (b). The reference and ground electrodes are located at the bottom-most position of the right and left ear-EEG electrodes, respectively.

2.3. Wearable ear-EEG headphone

The wearable ear-EEG equipment is designed in the shape of a headphone to avoid users feeling socially awkward when worn in daily life. The headphone case is printed with a 3D printer using polylactic (PLA) plastic as a material. The equipment can be easily worn due to the flexible headphone frame that is adjustable in size. The right cup of the headphone contains a Li-ion rechargeable battery (3000 mAh, lasts for at least eight hours for continuous EEG recording), a charger, a switch (to switch between operating mode and charging mode), and the OpenBCI's Cyton Biosensing Board (www.OpenBCI.com) which is used as the EEG acquisition board. The wearable device weighs approximately 400 gs. It is connected wirelessly to a personal computer via Bluetooth with a USB dongle. The ear-EEG is acquired with a sampling rate of 250 Hz. The headphone cups are 7×9 cm in size, which is large enough to cover the user's ears. A flexible silicone mold emblemed with sockets for snap-type electrodes is attached to the cushion of each headphone cup. Fig. 3 shows the prototype of the custom-made ear-EEG headphone.

The wearable ear-EEG headphone monitors EEG in eight channels positioned around the user's ears. For the sake of simplicity, we name four channels located around the left ear, from top to bottom, as L1, L2, L3, and L4, and the other four channels around the right ear as R1, R2, R3, and R4. The reference (REF) and ground (GND) electrodes are positioned below the R4 and L4 channels, respectively. Fig. 4 illustrates the positions of the ear-EEG electrodes. Foam-type solid-gel snap electrodes (3 M Red Dot 2239) cut to 14 mm in diameter are used in this study for EEG acquisition. This type of electrode is ready-to-use without the application of electrically conductive gel. They are soft and do not leave any unpleasant marks or scents on the user's skin. The electrodes have impedance below 15 kΩ and it remains at the same level throughout the experiment.

2.4. Experiment I: training session

The training session involves collecting subjects' ear-EEG data during their rest-condition and five different SI tasks, including SI of the words "power", "up", "down", "next", and "back". In this session of the experiment, subjects are shown an interactive simulation of a television that is displayed on a computer screen. There are five blocks of tasks in the experiment. Each block consists of five SI tasks (one for each word) and two rest tasks in a randomized order. Before each task, subjects are informed on which word to imagine, and how that SI task would affect the simulated television. The SI task of the word "power" would turn the simulated television on and off, the words "up" and "down" would change the volume of the television, and the words "next" and "back" would change the television channel. The volumes and channels of the television range from zero to ten. A real television sound is played from minimum to maximum volume with a 10% increase

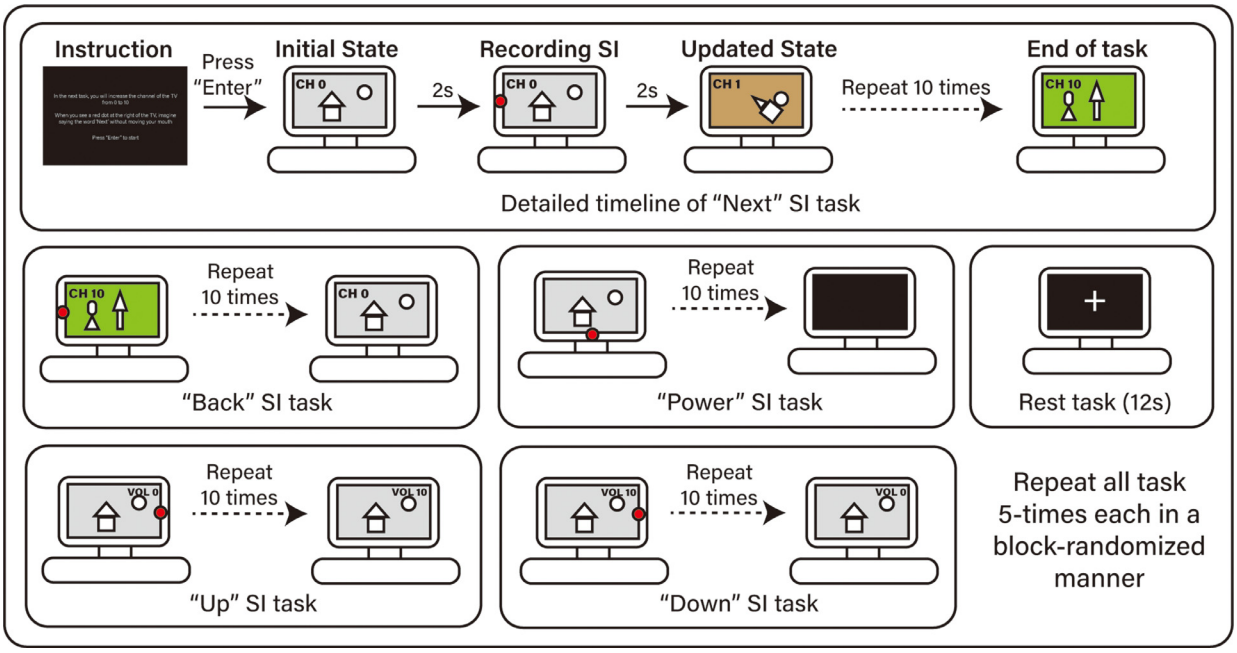

Fig. 5. Experimental procedure of Experiment I: training session. Five SI tasks: "Next", "Back", "Up", "Down", "Power", and a "rest" task were given in a block-randomized manner.

in volume for each level, and a distinct image is shown for each television channel. Depending on the instruction cue, subjects are told to look at a certain side of the television image ("power": bottom, "up" and "down": right, "next" and "back": left). A red focus circle is then shown in that region for two seconds, during which the subjects are instructed to perform the SI. The state of the television is then updated to reflect the SI. The same SI is carried out ten times consecutively in a SI task, with 2.5 s interim between each SI. Resting EEG data is collected by showing the subjects a fixation cross on a blank screen for twelve seconds. The first two seconds of the data are discarded when training the system. With this experimental procedure, we obtained 50 samples of EEG data for each SI and rest class. The procedure of Experiment I is illustrated in Fig. 5.

2.5. Data preprocessing

EEG data acquired from Experiment I are used to construct the classification models for the system. A 60 Hz notch filter is first applied to the whole data to remove the line noise. We then apply multiple bandpass filters to separate EEG signals into multiple time series lying in different frequency ranges. Seven fourth-order Butterworth bandpass filters ranging from 15 Hz to 120 Hz with an increment step and bandwidth of 15 Hz are used in this work. The frequency bands are chosen based on the offline analysis of our previous work which showed that the features from higher frequency ranges are the most significant ones in classifications of SI tasks [23]. The ear-EEG data are then segmented into 1.5-second EEG epochs and labeled with their corresponding class. CSP algorithm is then applied to the preprocessed EEG samples to spatially filter the data. This process is performed for data from each frequency band independently.

2.6. Feature extraction

2.6.1. Temporally-stacked multi-band covariance matrix

Features based on EEG covariance matrix have been shown in previous works to be effective in classifications of SI tasks [10,23]. EEG covariance matrix provides spatial information of an EEG epoch in the form of covariance values between each EEG channel. On the other hand, the spatiotemporal analysis of the EEG during SI tasks in previous works has shown distinctive temporal characteristics between different SI tasks. Thus, the incorporation of temporal information into the EEG covariance matrix is required to fully interpret the SI tasks from EEG data. To accomplish this, we introduce the temporally-stacked multi-band covariance matrix (TSMBC) method that includes all spatial, temporal, and spectral information to represent the neural activities during SI tasks. TSMBC method slices EEG epochs from multiple frequency bands into overlapping smaller windows and computes the covariance matrix separately for each window. The covariance matrices from each epoch are then subjected to further feature extraction steps before stacking them together as one feature vector that represents the EEG sample data.

Given an EEG sample in a time domain, $e \in \mathbb{R}^{CH \times T}$, where CH denotes the number of EEG channels and T denotes the number of time points, its covariance matrix, $P \in \mathbb{R}^{CH \times CH}$, is defined as:

$$P = \frac{1}{T-1} e e^{T}. \tag{1}$$

The covariance matrices are computed for all windows of all preprocessed EEG epochs acquired using the methods described in Section 2.5. In this work, the window-sliding procedure is performed with a window length of 1 s and a step length of 250 milliseconds, resulting in a total of three data windows for an EEG epoch. Since we use seven frequency bands, this procedure yields a total of twenty-one covariance matrices per one EEG sample. The resulting covariance matrices P are symmetric positive-definite (SPD).

2.6.2. Tangent space projection

The EEG covariance matrices representing each EEG epoch are projected into their corresponding tangent space before they can be used effectively as input features in the classification step. This approach is based on the Riemannian geometry of the SPD matrices, which causes them to be ineffective when they are vectorized

or used directly as features for classification algorithms based on projections into hyperplanes [24]. Tangent space projection is a local approximation of the Riemannian manifold. The resulting tangent space vectors from the projection are in Euclidean space and locally homeomorphic to the Riemannian manifold of the SPD matrices; thus, the Riemannian distance in the manifold of SPD matrices can be well approximated by computing the Euclidean distance between the tangent space vectors.

In this work, the Riemannian tangent space projections are calculated separately for each of the seven frequency bands. Each projection process is computed using the covariance matrices from all EEG windows of the training data samples. Given a covariance matrix P, its tangent space vector, $s \in \mathbb{R}^m$, where $m = \frac{CH(CH+1)}{2}$, is defined as:

$$s = upper\left(P_R^{-\frac{1}{2}} \log_{P_R}(P) P_R^{-\frac{1}{2}}\right). \tag{2}$$

The operator $upper(X)$ takes only the upper triangular part of the matrix X and vectorizes it by applying unity weight to the diagonal elements and $\sqrt{2}$ weight elsewhere. The operator $\log_{P_R}(P)$ is the logarithmic mapping of matrix P using the reference point P_R, defined as:

$$\log_{P_R}(P) = P_R^{\frac{1}{2}} log(P_R^{\frac{1}{2}} P P_R^{\frac{1}{2}}) P_R^{\frac{1}{2}} \tag{3}$$

where P_R is the Riemannian mean of the M covariance matrices, $\{P_1, P_2, ...P_M\}$, extracted from all EEG windows of the EEG epochs in the training dataset (i.e., M equals the number of EEG windows $\times$ the number of training EEG samples). In the current work, P_R is computed using the geometric mean [25] defined as follows:

$$P_R = \underset{P' \in \{P_1, P_2, ..., P_M\}}{argmin} \sum_{i=1}^{M} \delta_R^2\left(P', P_i\right). \tag{4}$$

The Riemannian distance, δ_R, between two SPD matrices is defined as:

$$\delta_R(P_1, P_2) = \log\left(P_1^{-1} P_2\right)_F = \left[\sum_{i=1}^{E} \log^2(\lambda_i)\right]^{\frac{1}{2}} \tag{5}$$

where λ_i is the ith eigenvalue of $P_1^{-1}P_2$. A detailed description of the Riemann geometry properties of the SPD matrices and the tangent space projection process can be found in [25].

To summarize our feature extraction process, one EEG sample is filtered into seven frequency bands, then the EEG epoch from each band is sliced into three overlapping windows. Consequently, the covariance matrix and its tangent space vector are calculated for each EEG window, resulting in a total of twenty-one (seven frequency bands $\times$ three EEG windows) tangent space vectors for one EEG sample. Because the number of EEG channels (CH) is eight, the number of features in a tangent space vector is thirty-six (from $m = \frac{CH(CH+1)}{2}$). The final feature vector representing an EEG epoch is then constructed by concatenating all twenty-one tangent space vectors, concluding the total feature number of 756 (twenty-one tangent space vectors $\times$ thirty-six features).

2.7. Classification

2.7.1. Multilayer extreme learning machine

Extreme learning machine (ELM) refers to a variation of a single layer feed-forward neural network (SLFN). In ELMs, the weights of the input layer and the bias values of the hidden layers are first randomly initialized, which are then frozen through the model training process [26]. Due to this, ELMs are much faster to train when compared to other neural networks while producing good generalization performance; hence, ELMs are well-suited for use in BCI systems which may require a frequent system calibration process considering the non-stationary nature of EEG signals.

For distinct samples (x_i, y_i), where $x_i = [x_{i1}, x_{i2}, ..., x_{in}]^T \in \mathbb{R}^n$, $y_i = [y_{i1}, y_{i2}, ..., y_{ic}]^T \in \mathbb{R}^c$, $i = 1, ..., N$, N is the number of training samples, n is the number of input nodes (i.e., the number of input features) and c is the number of output nodes (i.e., the number of output classes), an ELM with $\tilde{N}$ hidden nodes can be mathematically modeled as:

$$\sum_{j=1}^{\tilde{N}} v_j g\left(a_j x_i + b_j\right) = y_i \tag{6}$$

where $g(x)$ is the activation function, $j = 1, \ldots, \tilde{N}$, $v_j = [v_{j1}, v_{j2}, ..., v_{jc}]^T \in \mathbb{R}^c$ is the output weights connecting the j^{th}hidden node and the output nodes, $a_j = [a_{j1}, a_{j2}, ..., a_{jn}]^T \in \mathbb{R}^n$ is the input weights connection the j^{th}hidden node and the input nodes, and $b_j = [b_{j1}, b_{j2}, ..., b_{jn}]^T \in \mathbb{R}^n$ is the bias of the j^{th}hidden node. Considering all N training samples, the N number of Eq. (6) can be written compactly as

$$HV = Y \tag{7}$$

where

$$H = \begin{bmatrix} g(a_1 x_1 + b_1) & \cdots & g\left(a_{\tilde{N}} x_i + b_{\tilde{N}}\right) \\ \vdots & \ddots & \vdots \\ g(a_1 x_N + b_1) & \cdots & g\left(a_{\tilde{N}} x_N + b_{\tilde{N}}\right) \end{bmatrix}_{N \times \tilde{N}},$$

$$V = \begin{bmatrix} v_{11} & \cdots & v_{1c} \\ \vdots & \ddots & \vdots \\ v_{\tilde{N}1} & \cdots & v_{\tilde{N}c} \end{bmatrix}_{\tilde{N} \times c}, \text{ and } Y = \begin{bmatrix} y_{11} & \cdots & y_{1c} \\ \vdots & \ddots & \vdots \\ y_{N1} & \cdots & v_{Nc} \end{bmatrix}_{N \times c}.$$

H is called the hidden layer output matrix of the ELM where each column of H is the j^{th} hidden node output with respect to inputs $x_1, ..., x_N$. V is the output weight matrix containing all the output weights from each hidden node to output nodes. Y is the output matrix containing all N samples of the output nodes.

The process of training an ELM model is simple. First, the input weights a and bias b are randomly initialized to values between 0 and 1, from which we can derive the matrix H. We can then calculate the output weight as $V = H^t Y$ where H^t is the Moore-Penrose generalized inverse of the matrix H. By using input as output of the ELM network, we can construct an auto-encoding ELM (ELM-AE). ELM-AE models are trained identically to normal ELM models.

MLELM is a deep-learning variation of an ELM, which is implemented by stacking multiple ELM-AEs. It uses multiple ELM-AEs to train the input for each hidden layer [27]. Our previous work [23] has shown that MLELMs trained using Riemannian tangent space projections of EEG covariance matrices as input features outperform other methods commonly used in BCI systems in classification accuracy.

Given a MLELM model with k hidden layers, the l^{th} hidden layer is built with an ELM-AE that receives the output values of the $l-1^{th}$ hidden layer as input. The l^{th} hidden layer of a MLELM model can be expressed as:

$$H_l = g\left((V_l)^T H_{l-1}\right) \tag{8}$$

where H_l is the output matrix of the l^{th} hidden layer, V_l is the output weight matrix of the l^{th} hidden layer learned from the l^{th} ELM-AE. It should be noted that when $l = 1$, H_0 is the input layer of the MLELM model. The output weights that connect the last hidden layer to the output layer are then learned in the same manner as the original ELM. Please refer to [27] for detailed description on how a MLELM model is constructed.

2.7.2. Model training

To train the SI classification models for each subject, a five-fold cross-validation method is first applied to the data from Experiment I. There are three hidden layers in the MLELM models; a grid search method is applied to find the optimal number of hidden nodes in each hidden layer, ranging from 50 to 500 with an incremental step of 50. The CSP filters and the tangent space projections are trained using only training data in each iteration of the cross-validation. Three MLELM models are trained for each subject. The first model performs classification between the "rest" and "power" class, while the second and third models perform classification between "rest", "up" and "down", and "rest", "next" and "back", respectively. Since MLELM's performance can fluctuate depending on the random initialization of the parameters, random seed (from Python's NumPy library) is recorded to reproduce the same parameter initializations in the later step. After the cross-validation step, all three models are trained again using the optimal parameters and their corresponding random seed using the whole data from Experiment I.

2.8. System evaluation

In the previous sections, we have shown how the classification model is built to classify different SI tasks using the data obtained from Experiment I. The average classification accuracy of the five-fold cross-validation process is used to evaluate the offline performance of the system. To further evaluate the system in an online manner, we perform two more experiments: (1) an online test and model calibration experiment, and (2) a real-world scenario experiment. The online system evaluation is based on the classification accuracy of the trained model and its performance in specific tasks. After the experiments, survey questions regarding the SI tasks, our ear-EEG wearable device, the experiment, and the system protocol are also handed to the participants after they finish the experiments. The survey questions are designed to help us better understand how the system could be improved in the future. The survey questions are provided in Supplementary Material A. The objective and experimental protocol of each experiment are described in the following subsections.

2.8.1. Experiment II: online test and model calibration

After the model is trained using the training data, we carry out Experiment II to evaluate model performance in an online setting. The data acquired during the experiment is then used to further calibrate the model. Similar to Experiment I, a simulated television is shown, but with three green circles on the bottom, left and right sides of the television. In one session of Experiment II, participants are given six different types of tasks: increase or decrease the volume by one, increase or decrease the channel by one, turn on or turn off the television, and rest. The subjects are instructed with written words on a popup screen that participants can close by pressing the Enter key. To perform the instructed SI tasks, participants are told to move the mouse cursor (using normal mouse movement with a hand) into the corresponding green circle located at the right, left, and bottom of the television to indicate which mode of control they intend to perform: the right circle for volume control, the left circle for channel control, and the bottom circle for power control. When the cursor enters a circle, the color of the circle changes from green to red for two seconds. Subjects would then imagine the appropriate word to convey their desired command to the simulated television according to the given task while the circle remains red. EEG signals are collected during the first 1.5 s to be used in the classification of the user's intention. It should be noted that only the pre-trained MLELM model and algorithms (e.g., CSP filters and tangent space projection) which are corresponded to the selected mode of control are applied to the EEG signals. The state of the simulated television is adjusted according to the given task regardless of the classification result. Simple visual feedback (a checkmark or a cross mark) is then displayed for 500 milliseconds to inform the participants of the result for each task. For the rest task, participants are instructed to relax and watch the current state of the television continuously displayed for five seconds. The tasks are given randomly but the "Power" tasks are arranged so that the other SI tasks are not given while the simulated television is off. Each distinct task is performed for ten trials in one session of Experiment II.

After the participants finish a session of Experiment II, the true positive rate (TPR) of each task is reported. We then use the data obtained from the current session to calibrate our classification models. By using the grid search method, we find the new set of parameters that give the optimized classification accuracy for the new data. Finally, all models are retrained using both data from Experiment I and the current session of Experiment II. Experiment II is performed three times in total, with each session taking approximately nine minutes. Fig. 6 depicts the process of Experiment II. The average TPRs from the last session of Experiment II are used to measure the performance of the proposed online ear-EEG SI-based BCI system for each participant.

2.8.2. Experiment III: real-world scenario

Participants who achieve high performance in Experiment II are reinvited to participate in Experiment III to further evaluate the robustness of our system. Experiment III takes place after at least seven days from Experiment II. The objective of this experiment is to test the performance of the system in a real-world scenario. Furthermore, conducting Experiment III on a different day helps us test the generalizability and robustness of our models, which is an important property for systems that deal with a non-stationary signal such as EEG. Participants are first asked to carry out Experiment II once again using the pre-trained model from the previous session of Experiment II. The newly acquired online data are then used to recalibrate the models before performing the tasks in Experiment III. Unlike Experiment II, Experiment III is designed to allow participants to have complete control of the operations in the simulated television. Participants are given freedom over how they want to achieve their goal task. Participants control the interactive simulated television by moving the cursor into one of the three green circles; upon entry, the circle color changes to red, and the system starts translating the user's ear-EEG into the corresponding SI command. To reduce the false-positive rate, ear-EEG data of 1.5 s window is classified every 100 ms, and the final result command is output if and only if three consecutive classification results are identical. After an output command is produced, the state of the simulated television is changed accordingly, with 1.5 s interim before the next classification. Participants can freely move the cursor out of the focus circle to stop the current operation whenever they want as well.

In each trial of Experiment III, the simulated television is initially shown to be off. When the television is turned on, the channel and volume are set to five. There are two sub-tasks for the participants to perform. The first sub-task is to turn on the television, and then increase the volume and the channel to ten. The second sub-task is to decrease the volume and the channel back to its initial state of five and turn the television off. The participants are informed that they can freely choose the order of SI commands to accomplish the sub-tasks. Fig. 7 illustrates the procedure of Experiment III. The total session time, average command delivery time, the misstep number, and the total step number to achieve the goal are used as evaluation metrics; when calculating these metrics, the "rest" command is not considered as a command step due to the

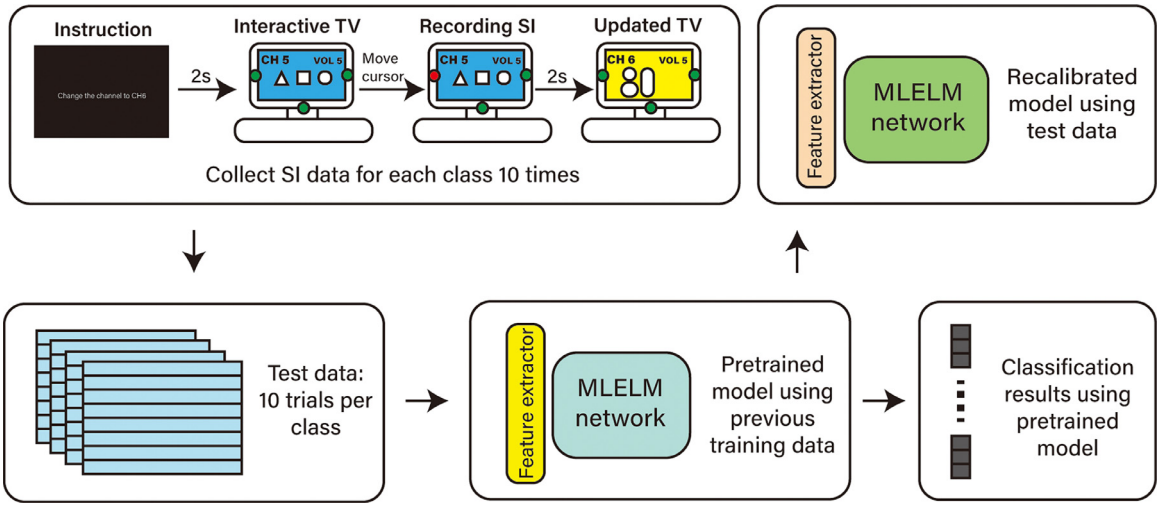

Fig. 6. Experimental procedure of Experiment II: online testing and model calibration session. The trained models are tested in an online experiment. The classification results are reported and the online-test data are used to calibrate the models to further improve the performance of the system.

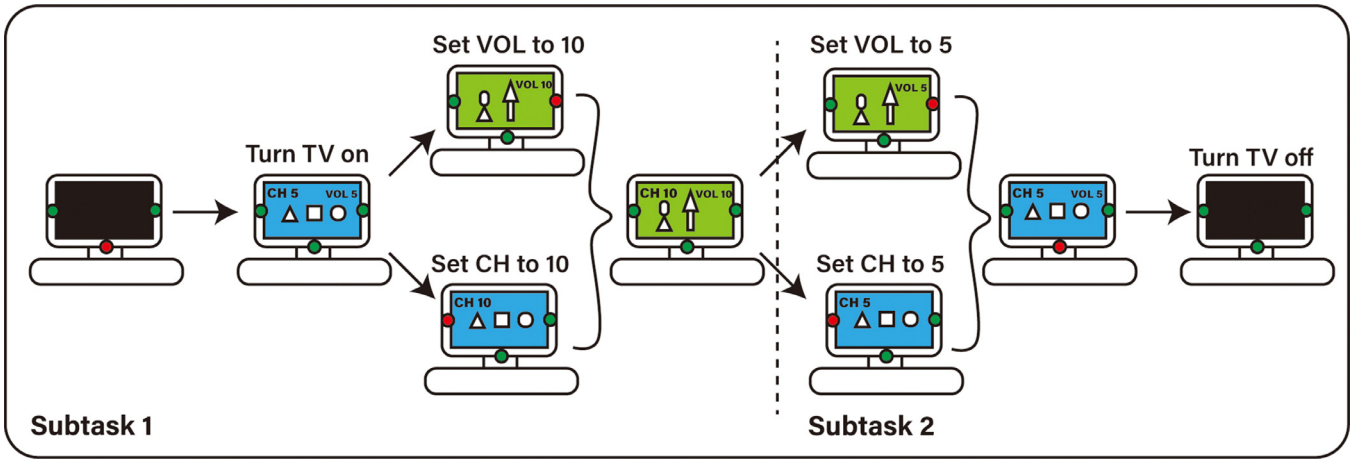

Fig. 7. Experimental procedure of Experiment III: real-world scenario session. Participants were given two sub-tasks to complete. The first subtask is to turn on the interactive simulated TV and change its channel and volume to ten. The second subtask is to change the channel and volume back to five and turn off the TV. Participants were given a complete control on how they want to finish the tasks.

fact that "rest" command does not affect the state of the simulated television. Experiment II and Experiment III are carried out consecutively for a total of three sessions to acquire a more accurate insight into the performance of our system.

3. Results and discussions

3.1. Experiment I: training session

Although the main objective of Experiment I is to gather data to train the models, the average classification accuracy from the offline cross-validation process can give us information on how well each participant performs the SI tasks. Table 1 shows the classification accuracies of each model (case 1 model classifies "power" and "rest" class, case 2 model classifies "up", "down", and "rest" class, and case 3 model classifies "next", "back", and "rest" class). From the results, all participants achieved the average classification accuracies significantly higher than the chance level (50% for case 1 model, 33.3% for case 2 and 3 models) according to the one-tailed t-test ($p < 0.01$) for all types of models. The average classification accuracies across all participants were 84.9%, 64.9%, and 64.5% for case 1, 2, and 3 models, respectively. Participant P2 performed exceptionally well among other participants with an average accuracy across all models of 97.9% while participant P8 performed the worst with an average accuracy of 55.9%.

3.2. Experiment II: online testing and calibration

Table 1 also shows the TPRs of each task during Experiment II which is used as an evaluation measure for the online performance. The average TPRs across all tasks of all participants for first, second and final sessions were 0.44, 0.45, and 0.59, respectively. Participant P2, who showed the best performance in the offline analysis of Experiment I, achieved the highest average TPR across all tasks (TPR = 0.85 in the last session) with TPR values higher than 0.5 in all tasks in the final session of Experiment II. In contrast, participant P5 showed the worst performance with an average TPR of 0.32 in the last session.

The result from Experiment II also shows an increase in online performance with more calibration process; the average TPR in the third session is significantly greater compared to the average TPR in the first session according to the one-way ANOVA ($p < 0.05$), with exceptions of participant P5 and P7 whose TPR decreased in the final session. There is no significant difference between the TPR

Table 1
The numerical results of Experiment I and Experiment II.

Partici-pant	Experiment I: Training session (acc%)			Experiment II: Online testing (TPR)							
	case 1	case 2	case 3	Session	Power	Up	Down	Next	Back	Rest	AVG
P1	100.0	87.3	76.0	#1	0.6	0.1	0.6	0.4	0.0	0.4	0.35
				#2	1.0	0.0	1.0	1.0	0.0	0.3	0.55
				#3	0.4	0.8	1.0	0.6	0.9	0.9	0.77
P2	99.0	98.7	96.0	#1	1.0	0.6	0.8	0.6	0.5	0.6	0.68
				#2	1.0	0.7	0.9	0.7	0.4	0.5	0.70
				#3	1.0	0.9	1.0	0.8	0.6	0.8	0.85
P3	70.0	52	50.7	#1	0.0	0.0	0.0	0.2	0.5	1.0	0.28
				#2	0.3	0.1	0.0	0.0	0.9	0.8	0.35
				#3	0.7	0.7	0.2	0.3	0.5	0.9	0.55
P4	89.0	63.3	69.3	#1	0.4	0.0	0.9	0.0	0.8	0.8	0.48
				#2	0.1	0.4	0.5	0.0	0.8	1.0	0.47
				#3	0.9	0.8	0.4	0.5	0.6	0.7	0.65
P5	75.0	52.0	50.7	#1	1.0	0.0	1.0	0.0	0.7	0.1	0.47
				#2	0.8	0.2	0.0	1.0	0.0	0.1	0.35
				#3	0.3	0.1	0.0	0.9	0.0	0.6	0.32
P6	81.0	53.3	59.3	#1	0.4	0.9	0.0	0.1	0.0	0.8	0.37
				#2	0.7	0.0	0.0	0.4	0.0	0.0	0.18
				#3	0.5	0.8	0.4	0.4	0.1	0.7	0.48
P7	67.0	50.0	51.3	#1	0.5	0.0	1.0	0.2	0.6	0.5	0.47
				#2	0.5	0.3	0.6	0.4	0.2	0.1	0.35
				#3	0.6	0.3	0.3	0.6	0.2	0.5	0.42
P8	71.0	48.7	48.0	#1	0.2	0.4	0.3	0.6	0.0	0.7	0.37
				#2	0.0	0.0	0.4	0.0	0.0	0.9	0.22
				#3	0.3	0.1	0.9	0.4	0.0	0.9	0.43
P9	90.0	75.3	62.0	#1	1.0	0.0	1.0	0.0	1.0	0.1	0.52
				#2	0.9	0.6	0.4	0.0	0.7	0.8	0.57
				#3	1.0	0.5	0.8	0.3	0.9	0.6	0.68
P10	92.0	56.7	58.0	#1	0.2	0.4	0.2	0.0	1.0	1.0	0.47
				#2	0.0	0.3	0.2	0.8	0.6	0.8	0.45
				#3	0.7	0.0	0.7	0.6	0.9	0.5	0.57
P11	100.0	76.7	88.7	#1	0.0	0.3	0.9	0.0	0.5	1.0	0.45
				#2	1.0	0.6	0.9	0.8	0.4	0.8	0.75
				#3	0.8	0.7	1.0	0.6	0.8	1.0	0.82
AVG	84.9	64.9	64.5	#1	0.48	0.25	0.60	0.19	0.51	0.64	0.44
				#2	0.57	0.29	0.45	0.46	0.36	0.55	0.45
				#3	0.65	0.52	0.61	0.55	0.50	0.74	0.59

Table 2
Results of Experiment III.

Participants	Session #	Online test and model calibration session (TPR)							Real-world scenario task					
		Task												
		Power	Up	Down	Next	Back	Rest	Average	Time (s)	#steps	#missteps	Time (s)	#steps	#missteps
P1	#1	0.5	0	0.9	0.1	0.8	1	0.55	–	–	–	50.37	11	0
	#2	1	0.6	1	0.7	0.5	0.9	0.78	49.95	13	1	58.59	15	2
	#3	1	1	0.9	1	0.6	0.8	0.88	131.14	23	6	53.45	15	2
P2	#1	1	0.9	1	1	1	0.5	0.90	58.01	15	2	61.28	17	3
	#2	1	0.5	1	1	0.8	1	0.88	49.41	13	1	52.12	15	2
	#3	1	0.9	0.6	0.6	0.5	1	0.77	52.60	13	1	42.71	11	0
P4	#1	0.7	0	1	1	0	1	0.62	73.60	17	3	–	–	–
	#2	0.8	0.1	0	0.5	0.7	1	0.52	–	–	–	–	–	–
	#3	0.5	0	1	0.1	0.4	1	0.50	–	–	–	–	–	–
P9	#1	0.1	0.1	0	0	0.1	1	0.22	–	–	–	–	–	–
	#2	0.3	0.5	0.4	0.2	1	0.9	0.55	119.57	21	5	–	–	–
	#3	0.8	0.8	0.1	0.4	0.2	0.7	0.50	178.34	39	14	138.08	17	3
P11	#1	1	0.8	0.7	0.4	0.9	0.6	0.73	78.67	17	3	–	–	–
	#2	0.1	0.9	0.4	0.8	0.7	0.8	0.62	60.00	15	2	69.30	15	2
	#3	1	0.9	0.3	0.7	1	0.5	0.73	–	–	–	–	–	–

of all SI tasks. Five participants including participants P1, P2, P4, P9, and P11 achieved an average TPR higher than 0.65 and were reinvited to participate in Experiment III.

3.3. Experiment III: real-world scenario

The results of Experiment III of the five participants (P1, P2, P4, P9, and P11) are shown in Table 2. Out of the five subjects, participants P2 and P11 achieved an average TPR higher than 0.65 in their first session of the online test without any model calibration process. Furthermore, participant P2 even outperformed their performance in the final session of Experiment II with an average TPR of 0.90 in the first online test session. Participant P1 outperformed their online testing result from Experiment II after the second calibration session. Participants P4 and P9 all showed performances lower than what they achieved in Experi-

ment II even after the calibration processes. Participant P1 showed an increase in online test performance with each calibration session while participants P2 and P4 showed a decreasing trend instead.

In the real-world scenario task, all subjects except for P4 completed both sub-task 1 and sub-task 2 for at least one session. Participant P2 succeeded in completing both sub-tasks in all three sessions and showed the best performance among all five participants. Participant P2 showed increased performance in the real-world scenario tasks after each calibration process, which was surprising given that their performance in the online testing part of the calibration session decreased instead with each session. The average performance time, the total number of steps and misstep number to finish a sub-task of participant P2 were 52.69 s, 14, and 1.5 missteps, respectively. The command delivery time was 3.79 s/command. Participants P1 and P11 completed both sub-tasks after the second calibration. However, participant P11 failed to finish both sub-tasks after the third calibration session while participant P1's performance got worse in the third session. The command delivery time of participants P1 and P11 were 3.88 and 4.31 command/seconds, respectively. Participant P9 successfully finished only sub-task 1 after the second calibration session, and finished both sub-tasks after the final calibration session but with very low performance: average performance time, the total number of steps, and misstep number of 158.21 s, 28, and 8.5, respectively. Participant P4 completed only sub-task 1 of the second session and failed all other subsequent tasks.

3.4. Discussions

Although the results from the experiments conducted in this study show that all participants achieved classification accuracy significantly higher than the chance level, only a few participants were able to achieve accuracy high enough to effectively control the interactive stimulated television in the real-world scenario tasks. Since most of the participants have prior experience in the SI-based BCI experiment, the reason for the difference between the individual performance appears to be independent of the user's experience. Possible explanations include individual anatomical and cortical differences that make neuro-activities during SI tasks poorly detectable by the wearable ear-EEG device. Further research is required to discover the exact reasons for the differences in user performance.

In Experiment III, the results show that two out of five participants achieved high TPRs in the online testing session that took place more than one week after Experiment I & II prior to any model calibration process. This suggests that, for these two participants, our system showed good robustness overall, maintaining high performance even after a period of time despite handling non-stationary EEG signals.

While the results from Experiment II show that the average TPR of the last session is significantly higher than the first session among all participants, there are some cases where the performance got worse as the calibration process progressed, especially in Experiment III. This might be due to bad EEG epochs from the newly obtained calibration data. The bad EEG epoch could be in form of an unexpected noise, motion artifact, or a user mistake while performing the task. As the calibration process tunes the models in favor of the newly acquired data, the calibrated models are more susceptible to poorly collected EEG samples, which leads to worse classification performances. Therefore, an additional process to check and remove the outliers from the calibration data is necessary to make sure that the models are accurately calibrated.

In our current online system, the optimal command delivery time is 3.2 s/command, assuming perfect classification. This time could be shortened by reducing the length of an EEG epoch, step size, and the interim between each output command to increase the control speed; however, such measures are likely to decrease the performance of the classification models. The tradeoff between the command delivery time and the accuracy is needed to be considered as well.

As seen in the experimental results, the proposed system is not yet ready to be used in a real-life scenario. Apart from the inadequate accuracy and command delivery speed, the current system also lacks a method to select the target object and/or mode of control. In this study, the experiments were conducted with participants manually moving a mouse cursor to select the mode of control of the simulated television. Ideally, this should be accomplished by SI tasks as well. Adding more SI classification modules to the system would allow us to have more levels of control. For example, there could be three levels of SI modules in which the first, second, and third module would be used to let the user select the target home appliance (e.g., "TV" or "Light" SI tasks), mode of control (e.g., "Volume" or "Channel" SI tasks), and control command (e.g., "Up" or "Down" SI tasks), respectively. Alternatively, different levels of control could also be done by other types of BCI components or a camera with an object recognition algorithm.

3.5. Survey results

In the first part of the survey, participants were asked questions regarding SI as a BCI paradigm. Participants were requested to score SI from 1 to 10 considering three different criteria: intuitiveness, ease of use, and how well focused they were while using SI. Participants from both BCI-experienced and inexperienced groups reported the SI tasks to be intuitive (average score of 8.4 and 7.0, respectively, with 10 being very intuitive). BCI-experienced participants responded that SI is easy to use (average score of 7.3 with 10 being very easy to use) and somewhat easy to keep their focus on the tasks throughout the experiment (average score of 6.4 with 10 being very easy to keep the focus). In contrast, the inexperienced group gave a neutral answer to both questions (average score of 5.5 and 5.0). These results indicate that SI tasks are intuitive and easy to use compared to other types of BCI. However, people with no experience in BCI systems may require some time to get familiar with the tasks.

The second part of the survey examines the participants' thoughts on the wearable ear-EEG device with respect to wearability, comfort, and applicability in real life. Most participants considered our device to be very easy to wear (average score of 8.6 with 10 being very easy). Participants also stated our device to be comfortable to wear at the start (average score of 8.2 with 10 being very comfortable), but less so at the end of the experiments (average score of 7.0). Three participants voted that they were not willing to wear the device in real life. These participants commented that the device was visually unappealing, causes sweating around the ears, and involved too much work to replace the electrodes every day. However, they also said that the device was much more comfortable to wear compared to the conventional scalp-EEG acquisition tool. We believe that the issue of the device's size and appearance can be easily fixed by customizing the biosensing board to reduce the size. The problem with perspiration may be solved by changing the material of the cushions or adding some holes around the headphone to increase the airflow. Lastly, the electrodes may be replaced with dry electrodes to solve the need for frequent replacement of electrodes, in return for a possible decrease in signal quality.

In the last part of the survey, we asked the participants questions related to experiment protocols and our system. The participants claimed that they were able to keep their focus throughout the experiment (average score of 7.6 with 10 being very focused)

and that they felt somewhat exhausted after the experiment (average score of 4.4 with 1 being very exhausted). When questioned about the time taken to acquire data and train the system, all participants said that 20 min (the approximate running time of Experiment I) was too long (average score of 9.0 with 10 being very long) to spend every day before using the system. They were then asked whether they were willing to spend 9 min (the approximate running time of Experiment II) at the start of each day before using the system for calibration instead. The participants still considered our model-calibration process to be too long (average score of 7.1). In response to the question about the upper limit of time for calibration for a real-life system that they were willing to use, we received an average answer of 3.1 min. All participants responded that the system was easy to understand and use (average score of 9.1 with 10 being very easy) but that they were not fully satisfied with the experience of using the system overall (average score of 6 with 10 being very satisfied). Seven participants answered that they would not use the system for controlling appliances in real life, primarily due to its low speed and accuracy. Nevertheless, they responded positively to using the system given that these issues were resolved.

Based on the survey answers, the major issues with our current systems are those involving preparation time and accuracy. One way to decrease the calibration time is to change the protocol of the calibration process. In this current study, Experiment II serves as both an online-testing session and a data gathering process for the model calibration; hence, the experimental protocol is designed to have a clear time margin between each task. For actual calibration, the time between each task can be greatly shortened by performing multiple numbers of an identical SI task consecutively similarly to Experiment I. The time used to display instructions can also be decreased as the user gets used to the system. Problems concerning accuracy require the development of better algorithms. Further research on how SI is generated in the brain is needed to better extract features that represent brain activities during SI tasks, which would allow us to select an appropriate classification model to best classify these features.

4. Conclusion

In this study, we proposed a novel online BCI system using a combination of SI tasks and a wearable ear-EEG headphone. In the offline analysis from Experiment I, we found that all participants were able to achieve classification accuracy significantly higher than the chance level. We also found promising results from the online experiments where a few participants were able to use the proposed system to control the simulated television with high accuracy and relatively fast command delivery time. Through a user survey, we found that participants were mostly satisfied with the SI-based BCI system and the wearable ear-EEG headphone and willing to use the system in real life given that the classification accuracy and command delivery time are improved. Answers to the survey questions also gave ideas and directions on how to further develop the ear-EEG SI-based BCI system. All things considered, we believe that the combination of the ear-EEG and SI tasks provides a powerful method of control for BCI systems that aims for daily-life use.

For future work, the development of better feature extraction and classification algorithms for SI tasks are required to increase the performance of the system. Noise-canceling and artifact-removal techniques should also be included in the system to ensure the quality of the EEG signal in a noisy real-world application scenario. Apart from developments in algorithms for the system, an embedded computing module or a connection between the device and the user's smartphone should be incorporated into the system to increase its mobility.

Declaration of Competing Interest

The authors declare the following financial interests/personal relationships which may be considered as potential competing interests:

Sungho Jo reports financial support was provided by Institute of Information and Communications Technology Planning and Grant funded by the Korea Government (MSIT) Evaluation (IITP) under Grant 2017-0-00432.

Acknowledgement

This work was supported by the Institute of Information and Communications Technology Planning and Evaluation (IITP) Grant funded by the Korea Government (MSIT) under Grant 2017-0-00432.

References

[1] T. Milekovic, A.A. Sarma, D. Bacher, J.D. Simeral, J. Saab, C. Pandarinath, B.L. Sorice, C. Blabe, E.M. Oakley, K.R. Tringale, E. Eskandar, Stable long-term BCI-enabled communication in ALS and locked-in syndrome using LFP signals, J. Neurophysiol. 120 (7) (2018) 343–360 Jul 1.
[2] M. Arican, K. Polat, Pairwise and variance based signal compression algorithm (PVBSC) in the P300 based speller systems using EEG signals, Comput. Methods Programs Biomed. 176 (2019) 149–157.
[3] N. Kaongoen, S. Jo, A novel hybrid auditory BCI paradigm combining ASSR and P300, J. Neurosci. Methods 279 (2017) 44–51 Mar 1.
[4] S. Chaudhary, et al., A flexible analytic wavelet transform based approach for motor-imagery tasks classification in BCI applications, Comput. Methods Programs Biomed. 187 (2020) 105325.
[5] J. Luo, et al., Motor imagery EEG classification based on ensemble support vector learning, Comput. Methods Programs Biomed. 193 (2020) 105464.
[6] L. Wang, et al., Analysis and classification of speech imagery EEG for BCI, Biomed Signal Process. Control 8 (6) (2013) 901–908.
[7] L. Friedman, J.T. Kenny, A.L. Wise, D. Wu, T.A. Stuve, D.A. Miller, J.A. Jesberger, J.S. Lewin, Brain activation during silent word generation evaluated with functional MRI, Brain Lang. 64 (2) (1998) 231–256 Sep 1.
[8] J.R. Binder, The Wernicke area: modern evidence and a reinterpretation, Neurology 85 (24) (2015) 2170–2175 Dec 15.
[9] L. Koessler, L. Maillard, A. Benhadid, J.P. Vignal, J. Felblinger, H. Vespignani, M. Braun, Automated cortical projection of EEG sensors: anatomical correlation via the international 10–10 system, Neuroimage 46 (1) (2009) 64–72 May 15.
[10] C.H. Nguyen, G.K. Karavas, P. Artemiadis, Inferring imagined speech using EEG signals: a new approach using Riemannian manifold features, J. Neural. Eng. 15 (2017) 016002.
[11] C.S. DaSalla, H. Kambara, M. Sato, Y. Koike, Single-trial classification of vowel speech imagery using common spatial patterns, Neural Netw. 22 (2009) 1334–1339.
[12] M. Matsumoto, J. Hori, Classification of silent speech using support vector machine and relevance vector machine, Appl. Soft Comput. 20 (2014) 95–102.
[13] S. Deng, R. Srinivasan, T. Lappas, M. D'Zmura, EEG classification of imagined syllable rhythm using Hilbert spectrum methods, J. Neural. Eng. 7 (2010) 046006.
[14] S. Martin, P. Brunner, I. Iturrate, J.D. Millán, G. Schalk, R.T. Knight, B.N. Pasley, Word pair classification during imagined speech using direct brain recordings, Sci. Rep. 6 (2016) 25803.
[15] M.N. Qureshi, B. Min, H.J. Park, D. Cho, W. Choi, B. Lee, Multiclass classification of word imagination speech with hybrid connectivity features, IEEE Trans. Biomed. Eng. 65 (2017) 2168–2177.
[16] J.S. García-Salinas, L. Villaseñor-Pineda, C.A. Reyes-García, A.A. Torres-García, Transfer learning in imagined speech EEG-based BCIs biomed, Signal Process. Control 50 (2019) 151–157.
[17] A.J. Casson, D.C. Yates, S.J. Smith, J.S. Duncan, E. Rodriguez-Villegas, Wearable electroencephalography, IEEE Eng. Med. Biol. Mag. 29 (3) (2010) 44–56 May 10.
[18] M.G. Bleichner, S. Debener, Concealed, unobtrusive ear-centered EEG acquisition: cEEGrids for transparent EEG, Front. Hum. Neurosci. 11 (2017) 163.
[19] V. Goverdovsky, et al., In-ear EEG from viscoelastic generic earpieces: robust and unobtrusive 24/7 monitoring, IEEE Sens. J. 16 (1) (2015) 271–277.
[20] P. Kidmose, D. Looney, M. Ungstrup, M.L. Rank, D.P. Mandic, A study of evoked potentials from ear-EEG, IEEE Trans. Biom. Eng. 60 (10) (2013) 2824–2830 May 29.
[21] J.W. Ahn, et al., Wearable in-the-ear EEG system for SSVEP-based brain–computer interface, Electron. Lett. 54 (7) (2018) 413–414.
[22] C. Athavipach, S. Pan-Ngum, P. Israsena, A wearable in-ear EEG device for emotion monitoring, Sensors 19 (18) (2019) 4014.
[23] N. Kaongoen, J. Choi, S. Jo, Speech-imagery-based brain–computer interface system using ear-EEG, J. Neural Eng. 18 (1) (2021) 016023.

[24] P. Gaur, et al., A multi-class EEG-based BCI classification using multivariate empirical mode decomposition based filtering and Riemannian geometry, Expert Syst. Appl. 95 (2018) 201–211.
[25] M. Moakher, A differential geometric approach to the geometric mean of symmetric positive-definite matrices, SIAM J. Matrix Anal. Appl. 26 (3) (2005) 735–747.
[26] G.-B. Huang, Q.-Y. Zhu, C.-K. Siew, Extreme learning machine: theory and applications, Neurocomputing 70 (1–3) (2006) 489–501.
[27] S. Ding, et al., Deep extreme learning machine and its application in EEG classification, Math. Probl. Eng. 2015 (2015).